

RESEARCH PAPER

Gallium Leaching from Fly Ash: A Mini-Review

Bagdaulet Kenzhaliyev¹; Ainur Berkinbayeva¹; Kenzhegali Smailov^{1,2}; Diana Karim^{1*}; Olga Atanova¹; Shynar Saulebekkyzy¹; Nazerke Tolegenova¹; Azamat Yessengazyev¹; Gulnur Abikenova³; Yerkem Birlirkhan¹

¹ Institute of Metallurgy and Ore Beneficiation JSC, Satbayev University, Almaty, Kazakhstan

² Al-Farabi Kazakh National University, Almaty, Kazakhstan

³ ERG Research and development, Almaty, Kazakhstan

*Corresponding author: d.karim@satbayev.university, tel.: +7(777)041-40-25, The Chemical Analytical Laboratory of the Institute of Metallurgy and Ore Beneficiation JSC, Satbayev University, Almaty 050013, Kazakhstan

Received: 05.03.2026

Accepted: 15.04.2026

ABSTRACT

Gallium (Ga) occurrence in coal is interpreted only by coupling bulk partitioning with microscale residence. Ga distribution reflects the allocation between inorganic matter and organics and correlates with ash yield. Al-bearing aluminosilicates dominate as hosts, with Ga retained mainly by isomorphic substitution governed by crystal chemistry rather than adsorption. Workflows compare where Ga sits versus how it is bound: density fractionation and sequential/selective leaching, constrained by XRD and supported by BSE-EDS, EMPA, and LA-ICP-MS. During combustion, Ga concentrates in fly ash/slag; recovery relies on pretreatment, acid leaching, and sorption/stripping, with calcination/roasting disrupting refractory frameworks, boosting extraction, and suppressing concurrent leaching of gangue elements.

Keywords: gallium (Ga), coal, aluminosilicates, isomorphic substitution, sequential leaching, thermal pretreatment.

INTRODUCTION

Gallium (Ga, Z = 31) is a Group 13 p-block element in the Periodic Table; its valence electrons occupy a p-subshell. Gallium rarely forms discrete mineral species instead, it occurs predominantly as an isomorphic trace constituent in aluminum- and zinc-bearing ores, as well as in coal. This geochemical mode of occurrence supports its classification as a dispersed metal, with typical average abundances on the order of 10–20 ppm [1].

Unlike most metals, gallium is often described as a molecular metal or a metallic molecular crystal, because its crystal structure combines molecular and metallic attributes. This duality is commonly rationalized by the tendency of Ga atoms to form covalently bonded Ga₂ dimers that are subsequently coupled through metallic bonding, with connectivity developing primarily within planes oriented perpendicular to the dimers mean position (Fig. 1) [2, 3].

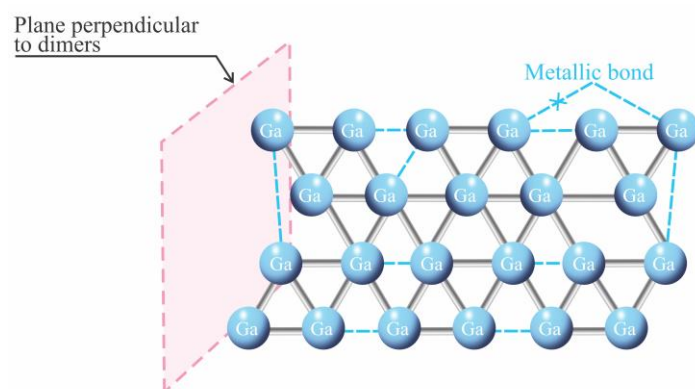


Fig. 1 Dimeric structure of Ga₂

These distinctive characteristics – together with low vapor pressure, pronounced chemical reactivity, and comparatively low toxicity – differentiate gallium from other liquid metals and alloys (e.g., mercury, cesium, and sodium-potassium alloys). As a consequence, gallium underpins value creation across multiple strategic manufacturing domains – ranging from electronics and automotive systems to aerospace and defense platforms, healthcare applications, and environmentally oriented technologies. In practice, Ga is used primarily as a platform material for integrated circuits (ICs) and optoelectronics, including

light-emitting diodes (LEDs), LiDAR components, space-qualified hardware, and laser diodes [4-7].

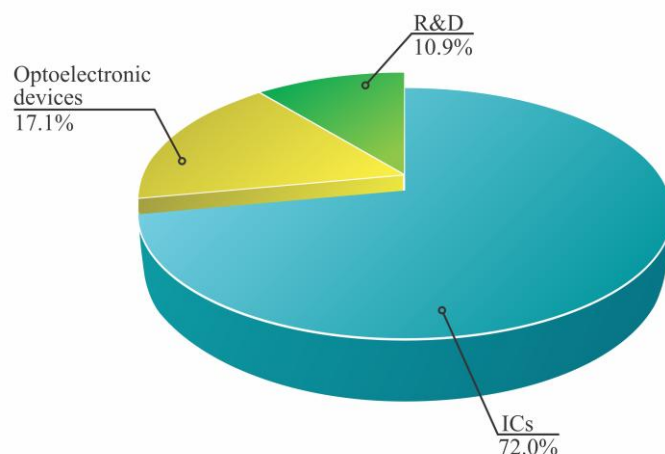


Fig. 2 Global gallium consumption by industrial sector

As shown in Fig. 2, global gallium demand is concentrated in high-technology industries. With integrated circuits (ICs) accounting for the largest share of demand (~72.0%), this sectoral breakdown is largely driven by the functional role of GaAs and GaN as compound-semiconductor platforms for RF electronics, telecommunications equipment, and high-performance computing architectures. A distant second position is occupied by optoelectronics (~17.1%). Here, the key product classes – LEDs, laser diodes, and photodetectors – depend on gallium-bearing active layers, and the segment remains structurally supported by growth in energy-efficient lighting, optical communication systems, and wider photonics deployment. The R&D segment (~10.9%) captures gallium consumption in research and engineering development activities that establish the technological base for subsequent expansion of downstream applications [8, 9].

For 2025–2030 (Fig. 3), the global gallium market is projected to expand from USD 28.7 to 40.8 billion, an absolute increase of USD 12.1 billion. This corresponds to a 42.8% rise relative to the baseline level. The expected growth is attributed to broader deployment of Ga-based semiconductor technologies in

global electronics and sustained demand for high-performance optoelectronic devices. Additionally, momentum arises from industry’s reassessment of the operational advantages of gallium compounds as device architectures become more complex. Component manufacturers are increasing the share of Ga-containing materials because, in several device classes, target specifications in frequency capability, energy efficiency, and reliability cannot be met without them [10, 11].

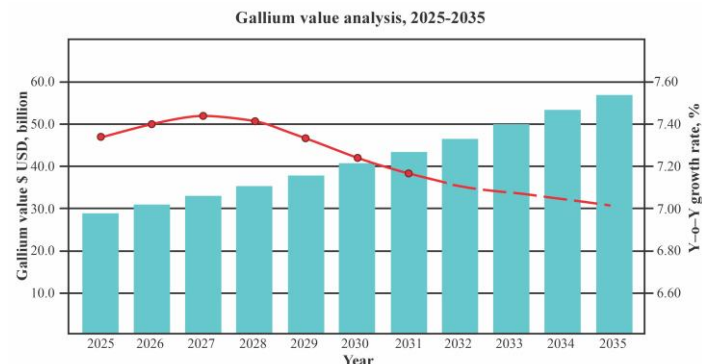


Fig. 3 Forecast of the global gallium market: price dynamics and CAGR

MATERIAL AND METHODS

Core gallium compounds and application material platform

In coal feedstocks, gallium is associated with both the inorganic fraction and the organic matter. It occurs as chemically bound and physically sorbed species, may be incorporated into pore-water components trapped within micropores and fractures, or can be adsorbed on the surface of the organic matrix. Establishing element occurrence modes typically requires a combined methodological framework that includes statistical data treatment, density fractionation, selective (sequential) leaching, X-ray diffraction (XRD), and a suite of microscopic, spectroscopic, and spectrometric techniques. Collectively, these approaches constrain the material’s structure and elemental – and in some cases isotopic-composition [12, 13].

The distribution of Ga in coal is heterogeneous and determined by coal genesis, lithology, and absolute concentration. Gallium may reside in either a polyminerall assemblage or the organic matrix. In most datasets, Ga shows a positive correlation with ash yield, implying predominant association with the inorganic phase – primarily with Al and aluminosilicates via isomorphic substitution for Al, and, to a lesser extent, with sulfide minerals (pyrite and sphalerite). Conversely, elevated Ga concentrations coupled with low ash yield are commonly interpreted as evidence for an organic affinity. Accordingly, Ga occurrence is often inferred from correlations with Al, Si, and S, as well as ash yield.

Sequential leaching enables quantitative partitioning of Ga among silicate, organic/sulfide, carbonate, Fe-Mn oxide, ion-exchangeable, and water-soluble fractions. Although applied relatively infrequently, the method has high diagnostic value. A more resolved picture is obtained from multiscale analyses performed directly on the native microstructural fabric of the specimen (BSE-EDS, EMPA mapping, LA-ICP-MS), which identify the microlocalization of trace elements and Ga-enriched domains within gel-like components of organic macerals [14-16].

Beyond its role in coal geochemistry, gallium is a critical raw material for a variety of high-tech applications – from III-V semiconductors like GaAs, GaN, and InGaN used in RF electronics, LEDs, and solar cells, to ultra-pure metallic gallium obtained as a by-product of alumina and zinc production. Table 1 provides an overview of the main gallium-based materials along with their processing routes and key technological challenges, illustrating why understanding how gallium occurs in primary sources matters for its efficient recovery and end use.

Table 1 Types of gallium compounds and their technological description [17-25].

Material	Form	Class	Processing context	Technologically relevant implications
Metallic gallium	Ga	Native metal (technological)	By-product of bauxite (Bayer process) and zinc hydrometallurgy	Very low melting point (29.8 °C) → easy purification by melting. Needs 5N-7N purity for electronics → multi-stage refining.
Gallium oxide	Ga ₂ O ₃	Oxides	Precipitation from Ga solutions + calcination	Intermediate for Ga purification. β-Ga ₂ O ₃ : high breakdown field, promising for power devices. Bulk crystals hard to grow.
Gallium arsenide	GaAs	III-V semiconductors	Epitaxial growth (MBE, MOCVD)	Direct bandgap, high electron mobility → RF, microwave, optoelectronics. Arsenic very toxic → strict safety rules.
Gallium nitride	GaN	III-V semiconductors (nitrides)	Heteroepitaxy on Si, SiC, sapphire	Wide bandgap → high-power, high-temperature operation. Key for LEDs, 5G, power electronics. High defect density is main problem.
Indium gallium nitride	InGaN	Ternary III-V semiconductors	Active layers in LEDs and laser diodes	Tunable bandgap → covers visible + UV light. Needs precise In content and strain control for LEDs/lasers.
Indium gallium arsenide	InGaAs	Ternary III-V semiconductors	Photodetectors, high-speed electronics	Narrow bandgap → IR detectors, high-speed transistors. Requires lattice-matched substrates → expensive.
Gallium phosphide	GaP	III-V semiconductors	Optoelectronics, substrates	Indirect bandgap → poor light emission efficiency. Used mostly in alloys or as substrate.
Ga-containing solar cells	GaAs, InGaP/GaAs/Ge	Multijunction semiconductors	Space hardware, concentrator photovoltaics	Extremely high cost limited to space, military, concentrator PV.

Gallium content in global coals

Gallium was identified in coal long before it gained industrial relevance. Its global average concentrations in coal are typically in the range of 1–10 ppm, although localized enrichments up to 20–30 ppm or higher have been reported for specific deposits. Determining the occurrence modes of gallium in coal (i.e., its speciation and host associations) is essential not only for constraining the element's sources and geochemical behavior during seam formation, but also for predicting its migration and partitioning during coal combustion, beneficiation, and processing. Such information is essential to evaluate gallium as a potentially valuable by-product stream. At present (Fig. 4), gallium recovery from coal and coal combustion by-products is pursued or under investigation in a number of countries, including Australia, Bulgaria, China, Egypt, Indonesia, Iran, Kazakhstan, Russia, South Africa, Spain, Tanzania, and Türkiye.

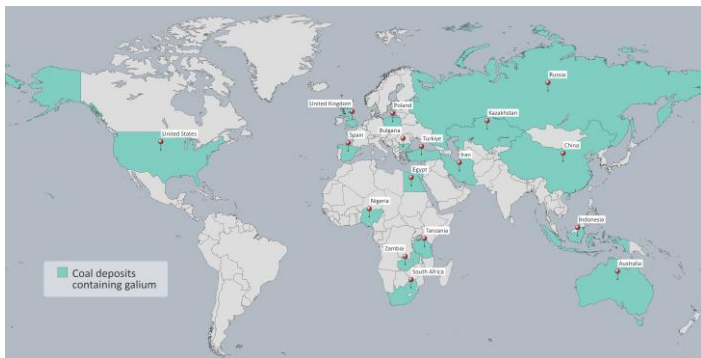


Fig. 4 Countries with gallium-bearing coal deposits

Gallium distribution is distinctly heterogeneous, both laterally across a seam and vertically through its thickness. This variability is controlled by coal-forming conditions, regional tectonic setting, the imprint of volcanogenic inputs, and related factors. Within the vertical profile of a seam, Ga concentrations can change markedly, roof and floor intervals frequently exhibit mean values that differ from those of the central part of the seam (Table 2) [26, 27].

Table 2 Average gallium content in coal-bearing ores [28–35].

Country	Mean concentration, ppm
Australia	14.00
Bulgaria	26.50
China	37.75
Egypt	6.50
Indonesia	5.40
Iran	10.90
Kazakhstan	6.08
Russia	7.00
South Africa	11.50
Spain	10.00
Tanzania	13.00
Türkiye	7.20

Methods for gallium recovery

Redistribution of gallium is a consistent feature of coal combustion: the element migrates away from the feed and becomes enriched in solid residues, with fly ash and bottom ash acting as the principal sinks. For hard (bituminous) coals, the corresponding ashes commonly exhibit higher Ga concentrations than ashes produced from brown (lignite) coals, a contrast attributable to differences in the starting fuel composition and, more specifically, in the character of the mineral matrix hosting Ga.

Boiler slag constitutes an additional by-product stream. In boiler configurations where bottom ash is held in a molten state prior to discharge, slag is generated as a granulated, non-combustible material dominated by a black, glassy phase, typically composed of particles up to a few millimeters. By concentration, Ga in boiler slag is reported at ~23 ppm, which is close to the level reported for bottom ash (~20 ppm) yet roughly twofold lower than in fly ash (~40 ppm) [36, 37].

Fly-ash-based recovery concepts therefore center on leaching routes designed to drive gallium into solution at high transfer efficiency. Notably, improved extraction is reported even under comparatively mild, less aggressive reagent regimes when pretreatment is applied to disrupt or weaken the inert ash matrix, thereby increasing the accessibility of structurally bound Ga. Process performance is governed by a compact set of operating variables: HCl concentration (1–8 M), liquid-to-solid ratio (2:6), contact time (2–30 h), temperature (25–65 °C), and particle size (from <0,105 mm to >0,21 mm). To reduce the impurity burden, the approach incorporated silica hydrolysis in an HCl medium, precipitation of Ca²⁺ as sulfate, and reduction of Fe³⁺ to Fe²⁺ (the specific reductant was not reported). Gallium was then recovered by optimizing sorption on polyurethane foam, evaluating the effects of chloride concentration (3–10 M), H₂SO₄ addition (up to 9 M), and temperature (4–55 °C), followed by water elution. On this basis, an integrated fly-ash processing scheme was proposed that yields a gallium chloride solution as the target product [38, 39].

Fig. 5 presents two alternative flowsheets for gallium recovery from coal fly ash, both beginning with HCl leaching and converging on a GaCl₃ solution as the final product. The left-hand route relies on sequential impurity removal (SiO₂, Ca²⁺, Fe³⁺) followed by gallium adsorption on polyurethane foam and water elution, while the right-hand scheme employs Fe³⁺ reduction with Na₂S, pH-controlled resin adsorption, and a solvent extraction-stripping cycle to achieve the same target product.

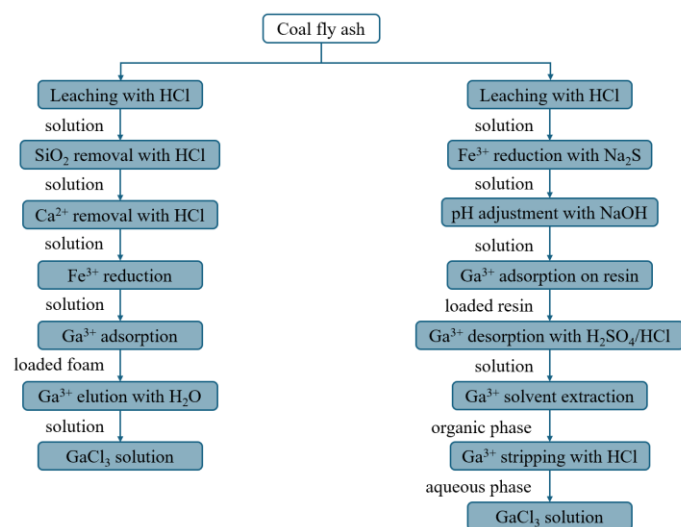


Fig. 5 Leaching-based recovery of gallium from coal ash

Understanding the occurrence modes of gallium in coal gangue constrains the choice of a hydrometallurgical recovery route, without such constraints, process design becomes essentially empirical. Aluminosilicates are the principal Ga hosts and are highly resistant to water, acids, and alkalis under ambient temperature and pressure. Direct leaching – including variants preceded by comminution in a planetary ball mill-using ammonium salt solutions (chlorides and/or sulfates) does not yield an acceptable transfer of Ga into solution. Comparable outcomes are reported for schemes that roast the gangue at 400 °C with ammonium salts followed by water leaching, dissolution remains low. Consistent Ga recovery therefore requires a dedicated pretreatment step performed under specifically selected conditions. This step should be treated as the process entry point because it disrupts the inert aluminosilicate matrix and increases Ga accessibility.

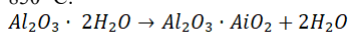
Table 3 illustrates how different pretreatment–leaching combinations affect gallium recovery from coal gangue. Single-step approaches, such as high-temperature roasting with sulfuric acid leaching, can achieve up to 95% yield, whereas milder calcination or multi-step routes involving intercalation and delamination tend to yield lower yields, confirming that the severity of matrix disruption is the key factor governing extraction efficiency.

Table 3 Optimal conditions for hydrometallurgical recovery of gallium from coal gangue [37-39].

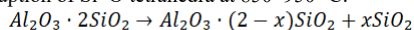
Pretreatment Stage	Leaching Conditions	Gallium Extraction
One-step pretreatment		
Calcination: 400 °C, 4h	2 M HCl, 60 °C, L/S 10, 4h	54%
Calcination: 400 °C, 2h	HNO ₃ (TD * 1:1), 170 °C, L/S 5, 2h	90%
Roasting: 650 °C, 2h	6 M H ₂ SO ₄ , 120 °C, L/S 10, 2h	95%
Roasting: (NH ₄) ₂ SO ₄ /CG (2.5:1), 450 °C, 2h	2 M HCl, 90 °C, L/S 10, 3h	90%
Roasting: Na ₂ CO ₃ /CG (1:1), 800 °C, 2h	2 M HCl, 90 °C, L/S 10, 3h	72%
Multi-step pretreatment		
I. Intercalation: CH ₃ COOK, 25 °C, 28h II. Delamination: H ₂ O, 0.5h, ultrasound, drying III. Roasting: (NH ₄) ₂ SO ₄ , 380 °C, 1h	H ₂ O, 70 °C, S/L 1:80, 1h, stirring	46%

Calcination is a process that alters the aluminosilicate matrix by disrupting its crystalline lattice. The transformation sequence comprises: [40, 41].

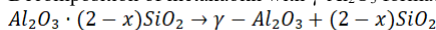
Kaolinite – metakaolinite via removal of structural and interlayer water at 450–850 °C:



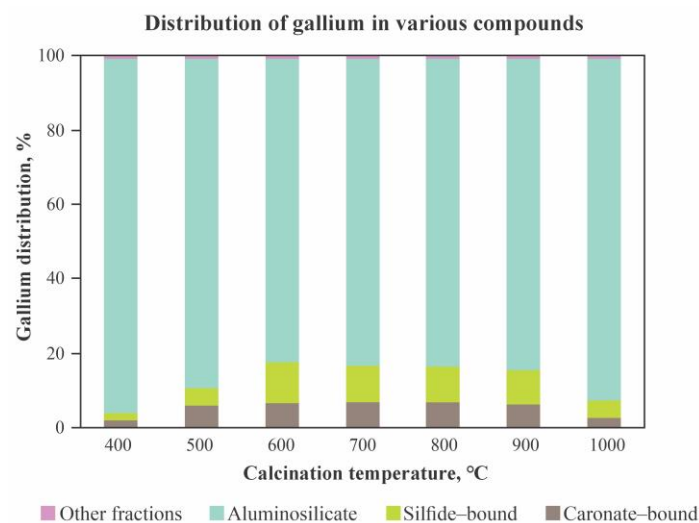
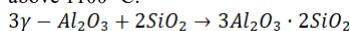
Subsequent disruption of Si–O tetrahedra at 850–950 °C:



Decomposition of metakaolin with γ -Al₂O₃ formation at 950–1100 °C:



Recombination of γ -Al₂O₃ with amorphous SiO₂ to form mullite at temperatures above 1100 °C:

**Fig. 6** Distribution of gallium in roasted coal gangue

Using sequential leaching, the authors tracked gallium transformations and its partitioning among operationally defined fractions as a function of roasting temperature (Fig. 6). The Ga share in the sulfide and carbonate fractions increases progressively and reaches a maximum in the 600–900 °C interval, while the contribution of the aluminosilicate-bound form decreases to 83 ± 1% (from 98 ± 1% in the untreated material and in the sample calcined at 1000 °C). The remaining forms—water-soluble, ion-exchangeable, and organic-associated –

collectively represent only a minor proportion (<0.7%). Such roasting-induced phase transformations can either enhance or suppress mineral solubility, thereby controlling the extent of Ga release during subsequent leaching [42-45].

CONCLUSION

Technologically, the mild routes surveyed – direct leaching in ammonium-salt media, or ammonium-salt roasting at 400 °C followed by water leaching – look attractive for practical reasons: the unit operations are straightforward, corrosion stress is plausibly lower, and reagent aggressiveness is reduced. The bottleneck is not operational, it is mineralogical. Gallium locked in refractory aluminosilicates dissolves poorly, so recovery plateaus early and scale-up value erodes.

Higher performance is consistently linked to a different logic. Thermal activation first (calcination/roasting), then acid leaching. Once the aluminosilicate lattice is disrupted or reconfigured, accessibility changes, and Ga transfer to solution can rise sharply – reaching ~90–95% under selected regimes. Predictability improves. The operating window becomes easier to steer. Costs shift elsewhere: energy demand increases at the high-temperature step, impurity co-dissolution typically intensifies and loads the leach liquor, and downstream purification/separation becomes non-optimal.

Integrated hydrometallurgical chains for fly ash (HCl leaching followed by impurity-reduction steps and polyurethane-foam sorption with water elution) are advantageous because they align directly with the production of a process liquor of gallium chloride (GaCl₃) and incorporate solution-conditioning blocks. The weaknesses are the multistage nature of the flowsheet, demands on materials of construction in chloride media, and the sensitivity of sorption performance to liquor composition. Future work should therefore prioritize optimization of activation (lower temperature and/or shorter residence time without sacrificing recovery), closure of reagent cycles, improved sorbent selectivity, and regime selection guided by a mechanistic understanding of Ga phase transformations during thermal treatment.

REFERENCES

- Ahrens, L. H. (1954). The lognormal distribution of the elements. *Geochimica et Cosmochimica Acta*, 6(2–3), 121–131. [https://doi.org/10.1016/0016-7037\(54\)90021-6](https://doi.org/10.1016/0016-7037(54)90021-6)
- Gong, X. G., Chiarotti, G. L., Parrinello, M., & Tosatti, E. (1991). α -gallium: A metallic molecular crystal. *Physical Review B*, 43, 14277–14280. <https://doi.org/10.1103/PhysRevB.43.14277>
- Gaston, N., & Parker, A. J. (2011). On the bonding Ga₂, structures of Ga_n clusters and the relation to the bulk structure of gallium. *Chemical Physics Letters*, 501, 375–378. <https://doi.org/10.1016/j.cplett.2010.11.006>
- Sun, W., Qi, M., Cheng, S., Li, C., Dong, B., & Wang, L. (2023). Gallium and gallium compounds: New insights into the “Trojan horse” strategy in medical applications. *Materials & Design*, 227, 111704. <https://doi.org/10.1016/j.matdes.2023.111704>
- Xiong, W. (2024). Advanced electronics: The emergence, evolution, and future of gallium nitride technology. *Transactions on Computational Science and Intelligent Systems Research*, 5, 693–697. <https://doi.org/10.62051/akz0c726>
- Frenzel, M., Mikołajczak, C., Reuter, M. A., & Gutzmer, J. (2017). Quantifying the relative availability of high-tech by-product metals – The cases of gallium, germanium and indium. *Resources Policy*, 52, 327–335. <https://doi.org/10.1016/j.resourpol.2017.04.008>
- Future Market Insights. (n.d.). Gallium market size and share forecast outlook 2025 to 2035. Retrieved February 9, 2026, from <https://www.futuremarketinsights.com/reports/gallium-market>
- Han, Z., Liu, Q., Ouyang, X., Song, H., Gao, T., Liu, Y., Wen, B., & Dai, T. (2024). Tracking two decades of global gallium stocks and flows: A dynamic material flow analysis. *Resources, Conservation & Recycling*, 202, 107391. <https://doi.org/10.1016/j.resconrec.2023.107391>
- Kenzhaliyev, B., Fischer, D., Temirova, S., Utlarukova, A., Baltabekova, Z., Bakhtuly, N., & Smailov, K. (2025). Removal of hexavalent chromium ions from industrial effluents using natural and modified diatomite, taurite, Lewatit M500, and activated carbon. *Processes*, 13(4), 997. <https://doi.org/10.3390/pr13040997>
- Shao, S., Ma, B., Wang, C., & Chen, Y. (2022). Extraction of valuable components from coal gangue through thermal activation and HNO₃ leaching.

- Journal of Industrial and Engineering Chemistry, 113, 564–574. <https://doi.org/10.1016/j.jiec.2022.06.033>
11. Berkinbayeva, A., Saulebekkyzy, S., Kenzhaliyev, B., Smailov, K., Yessengazyev, A., Nurtazina, N., Karim, D., & Birlikzhan, Y. (2025). Sodium percarbonate for eco-efficient cyanide detoxification in gold mining tailings. *Metals*, 15(10), 1162. <https://doi.org/10.3390/met15101162>
 12. Kenzhaliyev, B., Berkinbayeva, A., Baltabekova, Z., Moldabayeva, G., Smailov, K., Saulebekkyzy, S., Tolegenova, N., Karim, D., & Omirbek, T. (2025). Investigation of phase transformations in technogenic raw materials under microwave treatment for enhanced zinc leaching. *Processes*, 13(4), 1099. <https://doi.org/10.3390/pr13041099>
 13. Long, J., Zhang, S., & Luo, K. (2023). Discovery of anomalous gallium enriched in stone coal: Significance, provenance and recommendations. *Geoscience Frontiers*, 14, 101538. <https://doi.org/10.1016/j.gsf.2023.101538>
 14. Abdulvaliev, R. A., Surkova, T. Y., Baltabekova, Z. A., Yessimova, D. M., Stachowicz, M., Smailov, K. M., Dossymbayeva, Z. D., & Berkinbayeva, A. N. (2025). Effect of amino acids on the extraction of copper from sub-conditional raw materials. *Kompleksnoe Ispolzovanie Mineralnogo Syra = Complex Use of Mineral Resources*, 335(4), 50–58. <https://doi.org/10.31643/2025/6445.39>
 15. Dai, S., Finkelman, R. B., French, D., Hower, J. C., Graham, I. T., & Zhao, F. (2021). Modes of occurrence of elements in coal: A critical evaluation. *Earth-Science Reviews*, 222, 103815. <https://doi.org/10.1016/j.earscirev.2021.103815>
 16. Jiu, B., Jin, Z., & Wang, Z. (2023). Multiscale in-situ elemental characterization of critical elements in low-rank coal, implications for modes of occurrence. *Fuel*, 349, 128632. <https://doi.org/10.1016/j.fuel.2023.128632>
 17. Berkinbayeva, A., Kenzhaliyev, B., Smailov, K., Aimagambetov, A., Kamenov, B., Saulebekkyzy, S., Tolegenova, N., & Putri, P. S. R. (2025). An overview of biological cyanide elimination from tailing wastewater as a promising tool for sustainable utilization. *Water Research X*, 29, 100400. <https://doi.org/10.1016/j.wroa.2025.100400>
 18. U.S. Geological Survey. (2023, January). Gallium (Mineral Commodity Summaries 2023). Retrieved February 9, 2026, from <https://pubs.usgs.gov/periodicals/mcs2023/mcs2023-gallium.pdf>
 19. Sabot, J., & Luvray, H. (n.d.). Gallium and gallium compounds. In *Ullmann's Encyclopedia of Industrial Chemistry*. Wiley. Retrieved February 9, 2026, from <https://doi.org/10.1002/0471238961.0701121219010215.a01>
 20. Yuan, W., Chen, J., Teng, H., et al. (2021). A review on the elemental and isotopic geochemistry of gallium. *Global Biogeochemical Cycles*, 35(9), e2021GB007033. <https://doi.org/10.1029/2021GB007033>
 21. ASM International. (n.d.). ASM handbook (Vol. 2). Retrieved February 9, 2026, from <https://dl.asminternational.org/handbooks/edited-volume/61/Welding-Brazing-and-Soldering>
 22. Streetman, B., & Banerjee, S. (2014). *Solid state electronic devices* (7th ed.). Pearson. Retrieved February 9, 2026, from <https://www.pearson.com/en-us/subject-catalog/p/solid-state-electronic-devices/P200000003295>
 23. Fraunhofer Institute for Solar Energy Systems ISE. (n.d.). III–V solar cells. Retrieved February 9, 2026, from <https://www.ise.fraunhofer.de/en/business-areas/photovoltaics/iii-v-solar-cells.html>
 24. National Renewable Energy Laboratory. (n.d.). Multijunction solar cells. Retrieved February 9, 2026, from <https://www.nrel.gov/pv/multijunction-solar-cells.html>
 25. CRC Press. (n.d.). *CRC handbook of chemistry and physics* (Online ed.). Retrieved February 9, 2026, from <https://hbcpc.chemnetbase.com>
 26. Wang, W., Sang, S., Hao, W., Wang, R., Zhang, J., Duan, P., Qin, Y., & Xu, S. (2015). A cut-off grade for gold and gallium in coal. *Fuel*, 147, 62–66. <https://doi.org/10.1016/j.fuel.2015.01.066>
 27. Gladyshev, S., Akhmediyeva, N., Abdulvaliyev, R., Imangaliyeva, L., Smailov, K., Abikak, Y., Kasymzhanova, A., & Amanzholova, L. (2025). Utilization of red mud from processing of low-quality bauxites. *Processes*, 13(7), 1958. <https://doi.org/10.3390/pr1307>
 28. Zhang, Y., Wei, Y., Cao, D., Li, X., Wei, J., Xu, L., Dong, B., & Xu, T. (2024). Cooperative exploration of coal–gallium deposit. A case study of the Heidaigou coal–gallium deposit in the Jungar Coalfield, Inner Mongolia, China. *Minerals*, 14, 156. <https://doi.org/10.3390/min14020156>
 29. Hodgkinson, J. H., & Grigorescu, M. (2020). Strategic elements in the Fort Cooper Coal Measures: Potential rare earth elements and other multi-product targets. *Australian Journal of Earth Sciences*, 76, 305–319. <https://doi.org/10.1080/08120099.2019.1660712>
 30. Kenzhaliyev, B., Berkinbayeva, A., Smailov, K., Baltabekova, Z., Saulebekkyzy, S., Tolegenova, N., Yessengazyev, A., Bakhtyuly, N., & Tugambay, S. (2025). Microwave pre-treatment for efficient zinc recovery via acid leaching. *Materials*, 18(11), 2496. <https://doi.org/10.3390/ma18112496>
 31. Zhao, C., Qin, S., Yang, Y., Li, Y., & Lin, M. (2009). Concentration of gallium in the Permo–Carboniferous coals of China. *Energy Exploration & Exploitation*, 27, 333–343. <https://doi.org/10.1260/0144-5987.27.5.333>
 32. Kenzhaliyev, B., Surkova, T., Berkinbayeva, A., Baltabekova, Z., & Smailov, K. (2024). Harnessing microwave technology for enhanced recovery of zinc from industrial clinker. *Metals*, 14(6), 699. <https://doi.org/10.3390/met14060699>
 33. Anggara, F., Patria, A. A., Rahmat, B., Wibisono, H., Putera, M. Z. J., Petrus, H. T. B., Erviana, F., Handini, E., & Amijaya, D. H. (2024). Signature characteristics of coal geochemistry from the Eocene Tanjung Formation and the Miocene Warukin Formation, Barito Basin: Insights into geological control on coal deposition and future critical element prospecting. *International Journal of Coal Geology*, 282, 104423. <https://doi.org/10.1016/j.coal.2023.104423>
 34. Salikhov, V. A., Strakhov, V. M., & Yedibaev, A. I. (2021). Assessing the content of nonferrous and rare metals in nonclinking Kazakh coal. *Coke and Chemistry*, 64, 279–283. <https://doi.org/10.3103/S1068364X21070097>
 35. Kopobayeva, A., Baidautetova, I., Amangeldikyzy, A., & Askarova, N. (2024). *Geosciences*, 14, 143. <https://doi.org/10.3390/geosciences14060143>
 36. Kenzhaliyev, B., Surkova, T., Berkinbayeva, A., Baltabekova, Z., Smailov, K., Abikak, Y., Saulebekkyzy, S., Tolegenova, N., Omirbek, T., & Dosymbaeva, Z. (2025). Innovative methods for intensifying the processing of zinc clinker: Synergy of microwave treatment and ultrasonic leaching. *Metals*, 15(3), 246. <https://doi.org/10.3390/met15030246>
 37. Lu, F., Xiao, T., Lin, J., et al. (2017). *Hydrometallurgy*, 174, 105–115. <https://doi.org/10.1016/j.hydromet.2017.10.010>
 38. Huang, J., Wang, Y., Zhou, G., & Gu, Y. (2019). Investigation on the effect of roasting and leaching parameters on recovery of gallium from solid waste coal fly ash. *Metals*, 9, 1251. <https://doi.org/10.3390/met9121251>
 39. Zhang, L., Chen, H., Pan, J., Wen, Z., Shi, S., Long, X., & Zhou, C. (2022). The effect of physical separation and calcination on enrichment and recovery of critical elements from coal gangue. *Minerals*, 12, 1371. <https://doi.org/10.3390/min12111371>
 40. Wei, P., Wang, C., Wan, K., & Miao, Z. (2025). Study on recovering the scattered metals from coal gangue by low-temperature activation and two-stage selective leaching. *Separation and Purification Technology*, 357, 130214. <https://doi.org/10.1016/j.seppur.2024.130214>
 41. Ospanov, K., Smailov, K., & Nuruly, Y. (2020). Patterns of non-traditional thermodynamic functions Δ_rG^0/n and Δ_fG^0 (averaged) changes for cobalt minerals. *Chemical Bulletin of Kazakh National University*, 96(1), 22–30. <https://doi.org/10.15328/cb1005>
 42. Shao, S., Ma, B., Wang, C., & Chen, Y. (2022). Extraction of valuable components from coal gangue through thermal activation and HNO₃ leaching. *Journal of Industrial and Engineering Chemistry*, 113, 564–574. <https://doi.org/10.1016/j.jiec.2022.06.033>
 43. Kenzhaliyev, B., Koizhanova, A., Fischer, D., Magomedov, D., Yerdenova, M., Smailov, K., & Abdyldayev, N. (2025). Study of efficiency of organic activator application to process difficult-to-beneficiate polymetallic ridder ores. *Transition Metal Chemistry*, 50, 515–527. <https://doi.org/10.1007/s11243-025-00637-7>
 44. Kang, C., Yang, S., Qiao, J., Zhao, Y., Dong, S., Wang, Y., Duan, C., & Liu, J. (2024). Extraction of valuable critical metals from coal gangue by roasting activation–sulfuric acid leaching. *International Journal of Coal Preparation and Utilization*, 44, 1810–1827. <https://doi.org/10.1080/19392699.2023.2301311>
 45. Liu, Y., Yang, H., Sun, L., et al. (2024). Study on the occurrence of gallium in gallium-enriched coal gangue and migration during thermal treatment. *Journal of Sustainable Metallurgy*, 10, 1580–1593. <https://doi.org/10.1007/s40831-024-00876-5>